Polymer Journal (2015) 47, 158–163

www.nature.com/pj

ORIGINAL ARTICLE

Hydroxyapatite formation on oxidized cellulose nanofibers in a solution mimicking body fluid

Seira Morimune-Moriya[1,2], Sakina Kondo[1], Ayae Sugawara-Narutaki[1], Tatsuya Nishimura[3], Takashi Kato[3] and Chikara Ohtsuki[1]

Biomimetic processing using a solution mimicking the inorganic composition of the body fluid of humans (simulated body fluid (SBF)) may be one of the more promising routes for the construction of polymer/hydroxyapatite composites by an environmental-friendly method. In this process, hydroxyapatite nucleation on an organic polymer is an important event, yet the optimal surface characteristics of the organic polymer have not been determined. In the present study, a series of oxidized cellulose nanofibers with different contents of the carboxy groups (0–27% per glucose units of cellulose) were prepared. Their capability of forming hydroxyapatite in 1.5SBF (a solution in which the concentration of the inorganic ions was 1.5 times higher than that in SBF) was systematically investigated. It was found that hydroxyapatite formation on the nanofibers was the most enhanced with a nanofiber containing a carboxy group content of 9.9%, indicating that there was an optimum amount of carboxy groups that was required for the effective induction of hydroxyapatite nucleation. Carboxy groups are considered to be involved in the electrostatic interactions between the fibers and the calcium ions in solution and they induce heterogeneous nucleation of hydroxyapatite. Higher contents of carboxy groups, however, reduced the activity of the calcium ions for the nucleation of hydroxyapatite by forming complexes with the calcium ions.
Polymer Journal (2015) **47,** 158–163; doi:10.1038/pj.2014.127; published online 17 December 2014

INTRODUCTION

Recently, a huge variety in the combinations of organic and inorganic materials have been investigated to develop novel materials with unique performance capabilities, such as with their mechanical and optical properties.[1] These composites are expected to exploit the advantages derived from both the organic polymers and the inorganic materials.[2–5] In the organic/inorganic composites, problems regarding the mechanical performances have sometimes arisen due to poor interfacial adhesion between the organic and inorganic components. Poor interactions at the interface can easily cause an initial crack under the stress, which then fails to transfer the stress. Therefore, these composites often possess properties that are inferior to what was expected. To overcome this issue, many efforts have been made to increase the adhesive strength between the components.[3,6,7] Biomimetic processing is one such approach to fabricate novel organic/inorganic composites with highly organized structures with controlled interfacial properties.

Biominerals have attracted a great deal of attention as excellent organic/inorganic composites because of their highly organized structures.[8–12] These structures are constructed by a sophisticated process called biomineralization. Human bone tissue is a representative biomineral that consists of collagen and hydroxyapatite (HAp, stoichiometric composition of $Ca_{10}(PO_4)_6(OH)_2$), which contains carbonate.[11] Nacre of shell is composed of organic polymers, such as chitin and silk-fibroin-like proteins and calcium carbonate.[12] The organized structures of the biominerals comprised of organic and inorganic substances create unique properties, that is, the combination of the rigidity derived from the inorganic materials with the flexibility that is derived from the organic molecules. In addition, biomineralization occurs under ambient and mild conditions. Due to the superior properties of the biominerals combined with the environmental-friendly process of biomineralization, an enormous amount of effort regarding the bio-inspired composites have been made.[8,10,13–18]

Among the biomimetic processes, the technique for the coating of HAp onto organic substrates has been developed using an acellular aqueous solution. Kokubo *et al.*[19,20] developed an acellular aqueous solution that mimics the composition of the inorganic ions in human blood plasma for simulating HAp formation on bioactive glasses and glass-ceramics after implantation in bony defects. The solution is called simulated body fluid (SBF). SBF is evaluated to be supersaturated with respect to HAp.[21] SBF has been modified to create 1.5SBF, which is a solution with an increase in the inorganic concentrations of 1.5 times of the regular SBF, to increase the degree of supersaturation with respect to HAp for the coating of HAp on various substrates.[22] In the 1.5SBF solutions, functional groups on the surface of the substrate play important roles in the nucleation of HAp. Carboxy groups have been reported to effectively induce HAp

[1]Department of Crystalline Materials Science, Graduate School of Engineering, Nagoya University, Nagoya, Japan; [2]Venture Business Laboratory, Nagoya University, Nagoya, Japan and [3]Department of Chemistry and Biotechnology, School of Engineering, The University of Tokyo, Tokyo, Japan
Correspondence: Professor C Ohtsuki, Department of Crystalline Materials Science, Graduate School of Engineering, Nagoya University, Nagoya 464-8603, Japan.
E-mail: ohtsuki@apchem.nagoya-u.ac.jp
Received 22 September 2014; revised 16 November 2014; accepted 17 November 2014; published online 17 December 2014

nucleation on the surfaces of polyamide films that release calcium ions from the substrates.[23] The amount of carboxy groups in the polymer substrates affects the induction of the heterogeneous nucleation of HAp in 1.5SBF.[23] However, a systematic investigation on the effects of the carboxy groups in the system without the diffusion of calcium ions from the substrate has not yet been conducted.

Saito *et al.*[24] prepared composite films composed of calcium carbonate and cellulose nanofiber (CeNF), which was oxidized with carboxy groups. Based on their research for the designed CeNF, CeNFs with various amounts of carboxy groups could be fabricated to evaluate their roles and capabilities in the formation of HAp. Cellulose is the most abundant compound on earth and it is well known as an environmental-friendly material. CeNF would be a suitable component for nanocomposite materials as a potential reinforcement.[25–28] In this study, relationships between the amounts of carboxy groups formed on CeNFs and their capability of HAp formation in 1.5SBF were investigated.

MATERIALS AND METHODS

Materials

An aqueous suspension of CeNF (BiNFi-s cellulose, 2 wt%) was purchased from Sugino Machine, Uozu City, Japan. 2,2,6,6-Tetramethylpiperidine-1-oxyl radical (TEMPO) was purchased from Sigma-Aldrich (St. Louis, MO, USA). NaBr, NaClO and HCl were purchased from Wako Pure Chemical Industries, Ltd (Tokyo, Japan). NaOH, ethanol, NaCl, $NaHCO_3$, KCl, K_2HPO_4, $MgCl_2$, $CaCl_2$, Na_2SO_4 and tris(hydroxymethyl)aminomethane ($(CH_2OH)_3CNH_2$) were obtained from Nacalai Tesque, Inc (Kyoto, Japan). All of the reagents were used as received.

Oxidation of CeNF

An aqueous suspension of CeNF was diluted to 1 wt% and then the suspension (100 g) was stirred at room temperature for 1 day to obtain a homogeneous suspension. NaBr (0.2 g) and TEMPO (0.02 g) were dissolved into the suspension. NaClO (12%, x ml) was subsequently added to the suspension. The pH of the suspension was maintained at a value of 10 for 4 h by the dropwise addition of NaOH (0.5 M). After the oxidation reaction was allowed to occur for the designed period, ethanol was added to quench the oxidation. The suspension was then neutralized and washed with ultrapure water. The content of the carboxy groups introduced in the CeNF was controlled by the volume of NaClO ($x = 0$, 0.36, 2.16, 3.6, 7.2 ml).

Characterization of the oxidized CeNF

The presence of carboxy groups in the oxidized CeNF was confirmed by Fourier transform infrared (FT-IR) spectroscopy using a FT/IR-6100 (JASCO Co, Tokyo, Japan). The sample pellets were prepared using KBr. The concentration of the carboxy groups in the oxidized CeNF was determined by the electric conductivity titration method.[29] NaCl (0.01 M, 5 ml) was added to the suspension of the oxidized CeNF (0.5 wt%, 55 ml) and stirred to obtain a well-dispersed suspension. The pH of the suspension was adjusted to a value of 2.5–3.0 by adding HCl (0.1 M). Subsequently, a NaOH (0.04 M) solution was added at a rate of 0.1 ml min^{-1} to increase the pH to a value of 11. The content of the carboxy groups was determined from the conductivity and pH curves. An X-ray generator (RINT PC2100, Rigaku Co, Tokyo, Japan) was operated at 40 kV 20 mA^{-1}. X-ray diffraction profiles were obtained by irradiating the samples with CuKα radiation at a scanning speed of 1.0°·min^{-1}. The morphology of oxidized CeNF was observed using a field-emission scanning electron microscope (JSM-7500FA, JEOL Ltd, Tokyo, Japan). The samples were prepared by casting the diluted suspensions onto silicon wafers. Prior to the observations, the samples were coated with osmium.

Table 1 Reagents for preparation of 1.5SBF

Order	*Reagents*	*1.5SBF*
1	NaCl	11.994 g
2	$NaHCO_3$	0.525 g
3	KCl	0.336 g
4	$K_2HPO_4{\cdot}3H_2O$	0.342 g
5	$MgCl_2{\cdot}6H_2O$	0.458 g
6	HCl (1 mol l^{-1})	60 ml
7	$CaCl_2$	0.417 g
8	Na_2SO_4	0.107 g
9	$(CH_2OH)_3CNH_2$	9.086 g
10	HCl (1 mol l^{-1})	Appropriate amount for adjusting pH

Abbreviation: SBF, simulated body fluid.

Preparation of the oxidized CeNF film

The oxidized CeNF films were prepared by vacuum filtration. The suspension of oxidized CeNF (0.2 wt%, 150 g) was filtered using a polytetrafluoroethylene filter membrane (Advantec Toyo, Tokyo, Japan) with a 1.0 μm pore size. The obtained wet film was held between filter papers and glass plates and dried at 40 °C for 48 h. The film thickness was ~55 μm, and the film density was ~1.29 g cm^{-3}.

Preparation of 1.5SBF

The 1.5SBF was prepared by the method reported by Kokubo and coworkers.[22] NaCl, $NaHCO_3$, KCl, K_2HPO_4, $MgCl_2$, $CaCl_2$, Na_2SO_4, tris(hydroxymethyl)aminomethane ($(CH_2OH)_3CNH_2$) and HCl were added to ultrapure water (700 ml) in the order listed in Table 1. Each reagent was completely dissolved by stirring before the addition of the next reagent. The pH of the solution was buffered at 7.25 (36.5 °C) by $(CH_2OH)_3CNH_2$ and HCl. After cooling the solution to room temperature, the total volume of the solution was adjusted to 1000 ml by adding ultrapure water.

Evaluation of HAp formation

The oxidized CeNF film was cut into 1 × 1 cm squares and soaked in 1.5SBF (30 ml) at 36.5 °C for 1, 3, 5 and 7 days. The films were then removed from the 1.5SBF, rinsed with ultrapure water and dried at 40 °C for 24 h. The film surface was observed with a field-emission scanning electron microscope (JSM5600, JEOL Ltd). The samples were coated with a conductive layer of gold before observation. Concentrations of the calcium and phosphate in 1.5SBF before and after the soaking of the films were measured using inductively coupled plasma atomic emission spectroscopy (ICP-AES; Optima 2000DV, PerkinElmer Japan, Yokohama, Japan). To isolate only the precipitates, the soaked films were heated at 750 °C for 20 min to thermally decompose the cellulose. The residuals were characterized by X-ray diffraction within the range of 20–40°. All of the samples were scanned 12 times and the integrated intensities were obtained.

RESULTS

TEMPO-mediated oxidation of CeNF

The CeNF was oxidized by the TEMPO-mediated system to introduce carboxy groups onto the surface of the CeNF. The presence of the carboxy groups in the oxidized CeNF was confirmed by adsorption at 1660 cm^{-1} in the FT-IR spectra (Supplementary Figure S1). The content of the carboxy groups in the oxidized CeNF was controlled by the amount of NaClO used in the reaction. Table 2 shows the content of the carboxy groups in the oxidized CeNF as a function of the amount of NaClO (x). The content of the carboxy groups in the neat CeNF was revealed to be ~ 0, while for the oxidized CeNF the carboxy group content increased with a corresponding increase in the value of x. Hereafter, according to the content of the carboxy groups, the oxidized CeNF was termed as TyCeNF ($y = 1.3$, 9.9, 16, 27).

X-ray diffraction profiles of the TyCeNF are shown in Figure 1. The intensity peaks at $2\theta = 15°$, 16.4° and 22.6° were derived from the (1–10), (110) and (200) planes of cellulose I, respectively.[30]

Table 2 Carboxy group contents in CeNF and oxidized CeNF

NaClO x *(ml)*	*Carboxy group content (mmol g^{-1})*	*Carboxy group content*[a] y *(%)*
0	0	0
0.36	0.07	1.3
2.16	0.55	9.9
3.6	0.90	16
7.2	1.48	27

Abbreviation: CeNF, cellulose nanofiber.
[a]Carboxy group content per glucose unit.

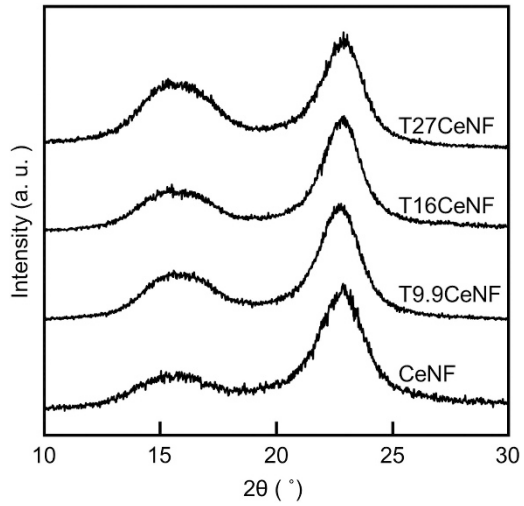

Figure 1 X-ray diffraction profiles of cellulose nanofiber (CeNF) and oxidized CeNFs.

The crystallinity of the cellulose was calculated as previously described in the literature and as follows:[31]

$$X_c = A_c/(A_a + A_c) \quad (1)$$

where, A_c is the crystalline area and A_a is the amorphous area. The X_c of CeNF decreased with an increase in the content of the carboxy group, and it decreased from 93% with neat CeNF to 84% with T27CeNF.

Figure 2 shows the field emission scanning electron microscope images of (a) CeNF, (b) T9.9CeNF, (c) T16CeNF and (d) T27CeNF. The dense network of the fibers was observed. It was found that the fiber morphology was maintained even after oxidation.

HAp formation in 1.5SBF

Figure 3a shows the scanning electron microscope images of CeNF and T*y*CeNF films before and after they were soaked in 1.5SBF. Spherical deposition was observed within 7 days for all of the T*y*CeNF films, while it was not observed for the CeNF film (0). As shown in Figure 3b, the deposition was composed of scale-like crystals. The morphology of the deposition is similar to that of HAp formed on substrates in 1.5SBF.[23,32,33] In previous reports, the deposition was assigned to bone-like HAp that was characterized as a carbonate-containing HAp comprised of small crystallites and defective structures. The deposition was formed within 1 day on the T9.9CeNF film, which was the fastest formation among the T*y*CeNF films. The induction period for the formation of deposition was shortened with an increase in the content of the carboxy groups up to 9.9%. However, the induction period was again prolonged with a continued increase in the content of the carboxy groups.

The concentration changes of the calcium and phosphorus in 1.5SBF that was measured by ICP-AES are shown in Figures 4a and b, respectively. The decrease in the concentration of calcium as well as

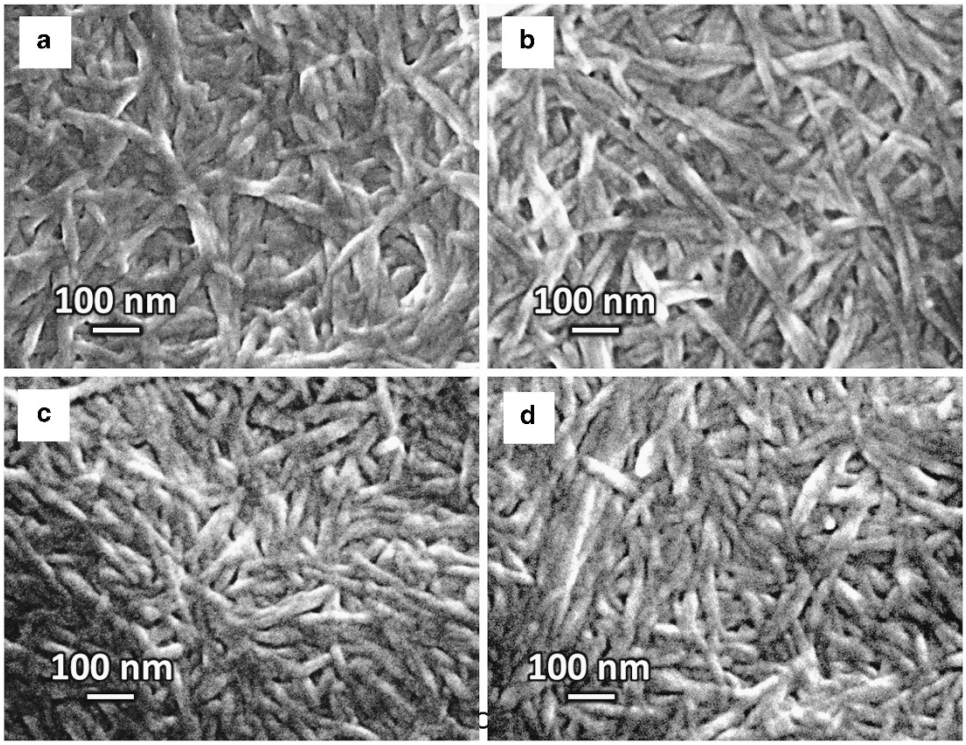

Figure 2 Field emission scanning electron microscope images of (**a**) cellulose nanofiber (CeNF), (**b**) T9.9CeNF, (**c**) T16CeNF and (**d**) T27CeNF.

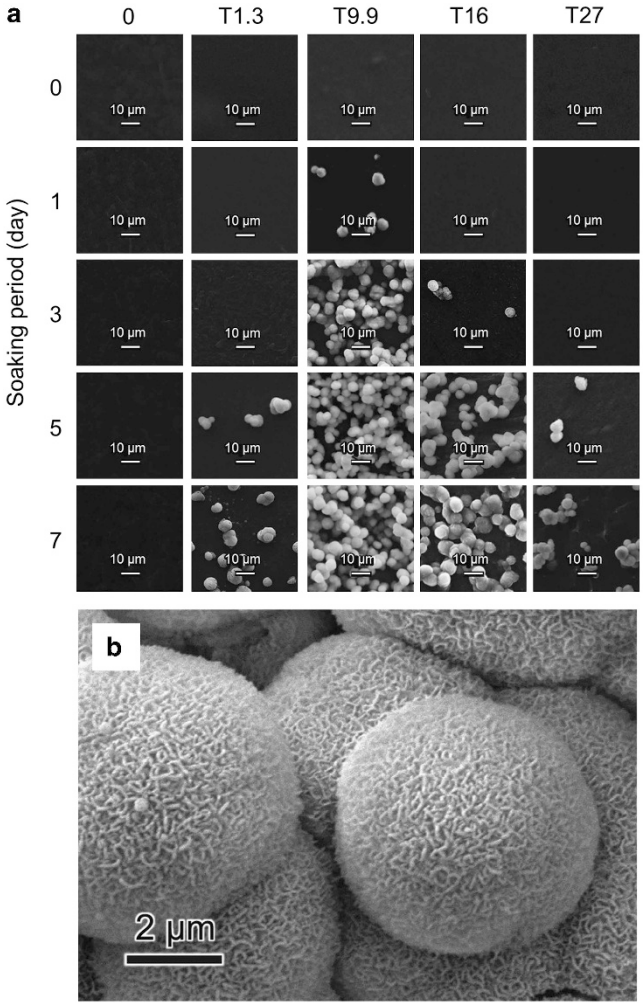

Figure 3 Scanning electron microscope images of (**a**) Cellulose nanofiber (CeNF) (0) and oxidized CeNF (T*y*) after soaking in 1.5SBF for 0–7 days and (**b**) T9.9CeNF after soaking in 1.5SBF for 7 days. T*y* indicates the oxidized film of CeNF with a carboxy group content of *y*.

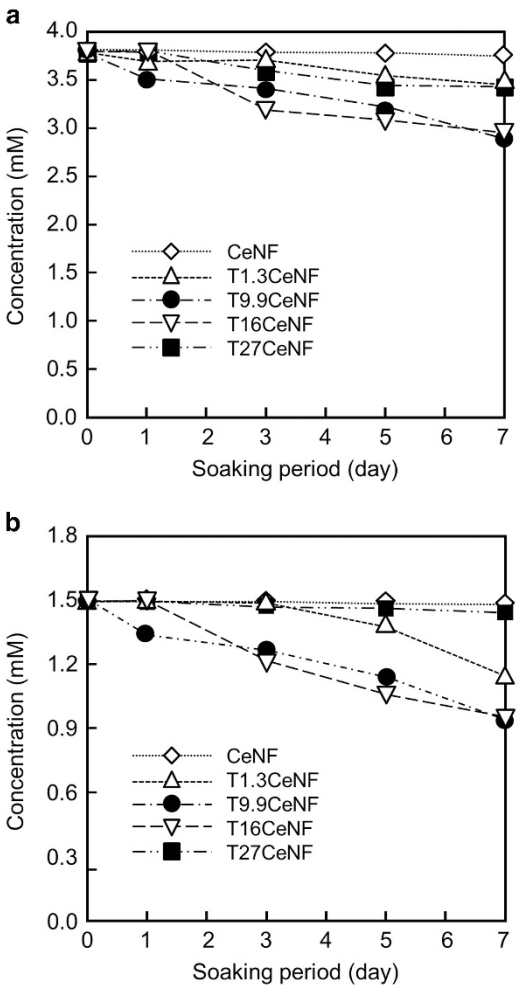

Figure 4 Concentrations of (**a**) calcium and (**b**) phosphorus as a function of the soaking period in 1.5SBF.

that of phosphorous was observed for the solutions where a deposition was formed. The deposition was determined to be calcium phosphate.

X-ray diffraction profiles of the T*y*CeNF soaked in 1.5SBF showed no distinct peaks of calcium phosphates; this can be attributed to the fact that the amount of inorganic deposits was so small compared with that of the T*y*CeNF substrates. Meanwhile, after the samples were heated to 750 °C, distinct peaks were observed in the X-ray diffraction profiles of the deposition on the T9.9CeNF films 3, 5 and 7 days after soaking in 1.5SBF, as shown in Figure 5. The diffraction peaks were assigned to a mixture of HAp and β-tricalcium phosphate ($Ca_3(PO_4)_2$). Since the samples were heated at 750 °C to thermally decompose the CeNF, the crystallinity of HAp can be higher than what was deposited in the 1.5SBF. Previously, Raynaud *et al.*[34] reported the thermal stability of HAp with a variable Ca/P atomic ratio. In their report, HAp with a Ca/P atomic ratio <1.5 was transformed into a mixture of HAp and β-tricalcium phosphate after heating at 700 °C, and was followed by a disappearance of HAp after heating at 750 °C. HAp with a Ca/P atomic ratio $=1.535$ (typical compositions possess a Ca/P atomic ratio between 1.5 and 1.67) dissociated into a mixture of HAp and β-tricalcium phosphate after heating at 700 and 750 °C. HAp powder with a Ca/P atomic ratio $=1.67$ was stable even after heating at 1000 °C. These findings on the thermal stability suggest that the heat-treated samples consisting of HAp and β-tricalcium phosphate were formed from HAp with a calcium-deficient composition ($Ca/P<1.67$) during the heating. Taking the aforementioned facts into consideration, the deposition formed on the T9.9CeNF in 1.5SBF was assigned to HAp.

DISCUSSION

Oxidation of CeNF

From the titration of T*y*CeNF, it was revealed that a series of oxidized CeNF with different contents of carboxy groups was successfully prepared. After the oxidation of CeNF, the X_c was found to decrease. It was suggested that the molecular weight of cellulose was slightly decreased due to the acid hydrolysis of the cellulose during the reaction.[35,36]

Capability of HAp formation in 1.5SBF

Regarding the HAp formation on the negatively charged surface in the series of SBF solutions, it has been reported that calcium ions initiate a heterogeneous nucleation of HAp.[33,37] Tanahashi *et al.*[37] investigated the effect of functional groups on the substrate surface on the formation of HAp in SBF. They prepared the substrates with methyl, phosphate, carboxy, amide, hydroxy and amino groups on the surfaces

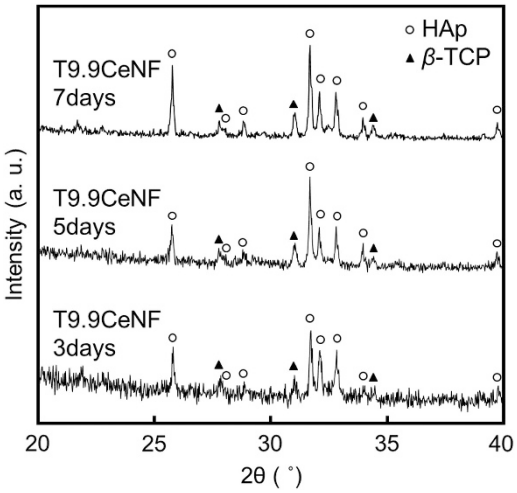

Figure 5 X-ray diffraction profiles of the deposits on the T9.9CeNF films 3, 5 and 7 days after soaking in 1.5SBF. The samples were heated at 750 °C for 20 min to thermally decompose the cellulose.

by using various alkanethiols on gold surfaces. The apatite growth rate was revealed to decrease in the following order: phosphate > carboxy ≫ amide ≃ hydroxy > amino ≫ methyl ≃ 0. This observation suggests that the adsorption of calcium ions on the negatively charged surface, rather than the adsorption of phosphate ions on the positively charged surface, dominates the first step of HAp formation. Due to this assumption, modification of a material surface to be a negatively charged surface has often been conducted to impart HAp formation capability in SBF.

Rhee *et al.*[33] used citric acid to promote HAp formation on a collagen membrane. The as-cast collagen membrane and the citric acid-treated collagen membrane were soaked in 1.5SBF. HAp crystals were observed on the treated membrane within 14 days, while they were not observed on the as-cast membrane. It was mentioned that negatively charged citric acid induced the HAp formation by initially binding the calcium ions. HAp formation was also induced on a cellulose cloth with the aid of citric acid in 1.5SBF.[38]

The neat cellulose showed a very low ability to form HAp, as seen by the fact that the deposition was not observed within 14 days. This shows that the hydroxy groups in the cellulose structure did not have the capability to form HAp in 1.5SBF during this period. However, deposition was observed for the oxidized CeNF. For the oxidized CeNF with a carboxy group content up to 9.9%, the induction period for HAp formation was shortened with an increase in the content of the carboxy groups. It was revealed that the carboxy groups in the oxidized CeNF had an important role in inducing the nucleation of HAp. Interestingly, the induction period was prolonged with a continued increase in the content of the carboxy groups past a content of 9.9%. The oxidized CeNF with the highest degree of oxidation at 27% was found to take 5 days for a deposition to form in the 1.5SBF solution while the deposition was observed within 1 day for the T9.9CeNF. The HAp formation on T*y*CeNF was not simply enhanced by an increase in the content of the carboxy groups, although some properties, such as the hydrophilicity and the swelling behavior of TyCeNF, would simply increase depending upon the content of the carboxy groups. This means that the ability of the fibers to form HAp was not significantly influenced by the hydrophilicity and swelling behavior of the samples.

Although the presence of optimum content of carboxy groups for HAp formation in 1.5SBF has been determined for the first time, the inhibitory effect of the carboxy groups on the formation of calcium phosphate has been known for the experimental system, where the degree of supersaturation of the solution to HAp was much higher than that in the 1.5SBF. Yokoi *et al.*[39] investigated the relationship between the carboxy groups in a polymer hydrogel and the formation of calcium phosphate. The copolymer hydrogels with different contents of carboxy groups were prepared by changing the molar ratios of acrylamide and acrylic acid; acrylamide/acrylic acid ratios were 100:0, 75:25, 50:50, 25:75 and 0:100. The mineralization of calcium phosphate was conducted by soaking the gel in a solution composed of calcium nitrate tetrahydrate and tris(hydroxymethyl) aminomethane. It was revealed that the increase in the content of the carboxy groups in the gel caused a decrease in the amount of the deposition. They explained that the activity of the calcium ions was decreased because the calcium ions were chelated by the carboxy groups, which were present in a high concentration in the gel. The diffusion of the calcium ions, as well as the nucleation, was inhibited by the chelation, reducing the HAp formation capability of the gel.

Chi *et al.*[40] also reported the inhibitory effect of the carboxy groups on the nucleation of calcium phosphate. They prepared calcium phosphate by mixing polyaspartic acids, sodium dihydrogen phosphate and calcium acetate solutions. To control the electrostatic interactions with the calcium ions, a series of polyaspartic acids with different contents of the carboxy groups were prepared by adjusting the hydroxylation degree of the polyaspartic acids. The formation of calcium phosphate was found to depend upon the degree of hydroxylation. The induction period for the calcium phosphate formation was prolonged with an increase in the carboxy group content from 0 to 85%. This indicates that the calcium ions were trapped at the surface of polyaspartic acid that was rich in the carboxy groups. A complex was formed by the negatively charged groups in the polyaspartic acid with the calcium ions, which greatly inhibited the nucleation of the calcium phosphate.

In our system, two competitive reactions were considered to have predominantly taken place in the 1.5SBF—the formation of a complex, including a chelate complex, and the nucleation of HAp. From the ICP-AES results, the calcium/phosphorus ratio was calculated using the concentration loss in 1.5SBF where the formation of HAp was observed. According to the stoichiometric ratios of HAp, the calcium/phosphorus ratio was expected to be ~1.67. However, the calcium/phosphorus ratio of 1.5SBF, where T27CeNF was soaked, was found to be >10. The decrease in calcium was observed for 1.5SBF where T27CeNF was soaked for 3 days, despite the fact that a deposition was not observed. Calcium ions may be more tightly bound to the surface of the T27CeNF by forming a 1:2 complex of the calcium ions with the carboxy groups in addition to the 1:1 complex because of the higher density of the carboxy groups in T27CeNF. This strong chelation results in the decrease of the activity of the calcium ions for nucleation. In contrast, the 1:1 complex formation may be dominant for T*y*CeNF with lower carboxy group contents ($y = 1.3$ and 9.9); calcium ions were more loosely bound to T*y*CeNF and thus were more active for nucleation. HAp formation was the most enhanced on T9.9CeNF because the calcium ions were effectively concentrated onto the surface in active states.

The X_c of T*y*CeNF may also affect HAp formation. Zhang *et al.*[41] mentioned that an increase in the X_c of a polymer substrate can facilitate the HAp formation in 1.5SBF. The degree and the size of the HAp deposition on poly(L-lactide) (semi crystalline polymer) and poly(D,L-lactide-co-glycolide) (amorphous polymer) were investigated. It was found that the HAp formation capability of poly(L-lactide) was slightly higher than that of poly(D,L-lactide-co-glycolide). In our

case, the X_c decreased from 93 to 84% with an increase in the carboxy group content from 0 to 27%, while the HAp formation was the most enhanced with T9.9CeNF having a moderate degree of crystallinity. Therefore, it was assumed that the differences in X_c may be a minor factor in the HAp formation in 1.5SBF.

CONCLUSION

In this work, we focused on determining the effects of the content of the carboxy groups in the oxidized CeNF on the HAp formation capability in 1.5SBF. CeNF was successfully oxidized by TEMPO-mediated oxidation and fibers with various contents of carboxy groups were prepared. The deposition of HAp was observed within 5 days, 1 day, 3 days and 5 days for the oxidized CeNF with carboxy group contents of 1.3%, 9.9%, 16% and 27%, respectively, which indicates that there is an optimal content of carboxy groups (9.9%) that effectively induces HAp formation. The lack of electrostatic interactions and also the excess electrostatic interactions between the carboxy groups of the oxidized CeNF and the calcium ions in 1.5SBF may cause the delay in the HAp formation. A thorough understanding of the effects of the carboxy groups, including the position and the distance on the substrate,[42] in addition to the present findings will lead to the development of fusion materials with highly organized CeNF/HAp composite structures.

ACKNOWLEDGEMENTS

This work was supported by a Grant-in-Aid for Scientific Research (No. 22107003, 22107005 and 22107007) on the Innovative Areas of 'Fusion Materials: Creative Development of Materials and Exploration of Their Function through Molecular Control' (No. 2206) from the Ministry of Education, Culture, Sports, Science and Technology, Japan (MEXT).

1 in: *Nanocomposite Science and Technology* (eds Ajayan, P. M., Schadler, L. S., Braun. P. V.) (Wiley-VCH, Weinheim, Germany, 2003).
2 Usuki, A., Kojima, Y., Kawasumi, M., Okada, A., Fukushima, Y., Kurauchi, T. & Kamigaito, O. Synthesis of nylon 6-clay hybrid. *J. Mater. Res.* **8**, 1179–1184 (1993).
3 Chujo, Y. & Tamaki, R. New preparation methods for organic–inorganic polymer hybrids. *MRS Bull.* **26**, 389–392 (2001).
4 Yamamoto, Y., Nishimura, T., Saito, T. & Kato, T. $CaCO_3$/chitin-whisker hybrids: formation of $CaCO_3$ crystals in chitin-based liquid-crystalline suspension. *Polym. J.* **42**, 583–586 (2010).
5 Morimune, S., Nishino, T. & Goto, T. Poly (vinyl alcohol)/graphene oxide nanocomposites prepared by a simple eco-process. *Polym. J.* **44**, 1056–1063 (2012).
6 Nishino, T. & Arimoto, N. All-cellulose composite prepared by selective dissolving of fiber surface. *Biomacromolecules* **8**, 2712–2716 (2007).
7 Jing, H., Higaki, Y., Ma, W., Xi, J., Jinnai, H., Otsuka, H. & Takahara, A. Preparation and characterization of polycarbonate nanocomposites based on surface-modified halloysite nanotubes. *Polym. J.* **46**, 307–312 (2014).
8 Mann S. in *Biomineralization–Principles and Concepts in Bioinorganic Materials Chemistry* (eds Compton, R.G., Davies, S.G., Evans, J.) (Oxford University Press, New York, 2001).
9 Weiner, S. & Addadi, L. Design strategies in mineralized biological materials. *J. Mater. Chem.* **7**, 689–702 (1997).
10 Meldrum, F. C. & Cölfen, H. Controlling mineral morphologies and structures in biological and synthetic systems. *Chem. Rev.* **108**, 4332–4432 (2008).
11 Weiner, S. & Wagner, H. D. The material bone: structure-mechanical function relations. *Annu. Rev. Mater. Sci.* **28**, 271–298 (1998).
12 Weiner, S., Traub, W. & Parker, S. B. Macromolecules in mollusc shells and their functions in biomineralization. *Philos. Trans. R. Soc. Lond. B* **304**, 425–434 (1984).
13 Sugawara-Narutaki, A. Bio-inspired synthesis of polymer-inorganic nanocomposite materials in mild aqueous systems. *Polym. J.* **45**, 269–276 (2013).
14 Kato, T. & Amamiya, T. A new approach to organic/inorganic composites. Thin film coating of $CaCO_3$ on a chitin fiber in the presence of acid-rich macromolecules. *Chem. Lett.* **28**, 199–200 (1999).
15 Sugawara, A., Nishimura, T., Yamamoto, Y., Inoue, H., Nagasawa, H. & Kato, T. Self-organization of oriented calcium carbonate/polymer composites: effects of a matrix peptide isolated from the exoskeleton of a crayfish. *Angew. Chem. Int. Ed.* **45**, 2876–2879 (2006).
16 Obara, S., Yamauchi, T. & Tsubokawa, N. Evaluation of the stimulus response of hydroxyapatite/calcium alginate composite gels. *Polym. J.* **42**, 161–166 (2010).
17 Wang, Y., Azaïs, T., Robin, M., Vallée, A., Catania, C., Legriel, P., Pehau-Arnaudet, G., Babonneau, F., Giraud-Guille, M.-M. & Nassif, N. The predominant role of collagen in the nucleation, growth, structure and orientation of bone apatite. *Nat. Mater.* **11**, 724–733 (2012).
18 Kochumalayil, J. J., Morimune, S., Nishino, T., Ikkala, O., Walther, A. & Berglund, L. A. Nacre-mimetic clay/xyloglucan bionanocomposites: a chemical modification route for hygromechanical performance at high humidity. *Biomacromolecules* **14**, 3842–3849 (2013).
19 Kokubo, T., Kushitani, H., Sakka, S., Kitsugi, T. & Yamamuro, T. Solutions able to reproduce *in vivo* surface-structure changes in bioactive glass-ceramic A-W. *J. Biomed. Mater. Res.* **24**, 721–734 (1990).
20 Cho, S.-B., Nakanishi, K., Kokubo, T., Soga, N., Ohtsuki, C., Nakamura, T., Kitsugi, T. & Yamamuro, T. Dependence of apatite formation on silica gel on its structure: effect of heat treatment. *J. Am. Ceram. Soc.* **78**, 1769–1774 (1995).
21 Ohtsuki, C., Kokubo, T. & Yamamuro, T. Mechanism of apatite formation on CaO-SiO_2-P_2O_5 glasses in a simulated body fluid. *J. Non Cryst. Solids* **143**, 84–92 (1992).
22 Abe, Y., Kokubo, T. & Yamamuro, T. Apatite coating on ceramics, metals and polymers utilizing a biological process. *J. Mater. Sci. Mater. Med.* **1**, 233–238 (1990).
23 Miyazaki, T., Ohtsuki, C., Akioka, Y., Tanihara, M., Nakao, J., Sakaguchi, Y. & Konagaya, S. Apatite deposition on polyamide films containing carboxyl group in a biomimetic solution. *J. Mater. Sci. Mater. Med.* **14**, 569–574 (2003).
24 Saito, T., Oaki, Y., Nishimura, T., Isogai, A. & Kato, T. Bioinspired stiff and flexible composites of nanocellulose-reinforced amorphous $CaCO_3$. *Mater. Horiz.* **1**, 321–325 (2014).
25 Henriksson, M., Berglund, L. A., Isaksson, P., Lindström, T. & Nishino, T. Cellulose nanopaper structures of high toughness. *Biomacromolecules* **9**, 1579–1585 (2008).
26 Sehaqui, H., Mushi, N. E., Morimune, S., Salajkova, M., Nishino, T. & Berglund, L. A. Cellulose nanofiber orientation in nanopaper and nanocomposites by cold drawing. *ACS Appl. Mater. Interfaces* **4**, 1043–1049 (2012).
27 Sehaqui, H., Morimune, S., Nishino, T. & Berglund, L. A. Stretchable and strong cellulose nanopaper structures based on polymer coated nanofiber networks. *Biomacromolecules* **13**, 3661–3667 (2012).
28 Fujisawa, S., Saito, T., Kimura, S., Iwata, T. & Isogai, A. Surface engineering of ultrafine cellulose nanofibrils toward polymer nanocomposite materials. *Biomacromolecules* **14**, 1541–1546 (2013).
29 Saito, T. & Isogai, A. TEMPO-mediated oxidation of native cellulose. The effect of oxidation conditions on chemical and crystal structures of the water-insoluble fractions. *Biomacromolecules* **5**, 1983–1989 (2004).
30 Qi, H., Cai, J., Zhang, L. & Kuga, S. Properties of films composed of cellulose nanowhiskers and a cellulose matrix regenerated from alkali/urea solution. *Biomacromolecules* **10**, 1597–1602 (2009).
31 Kljun, A., Benians, T. A. S., Goubet, F., Meulewaeter, F., Knox, J. P. & Blackburn, R. S. Comparative analysis of crystallinity changes in cellulose I polymers using ATR-FTIR, X-ray diffraction, and carbohydrate-binding module probes. *Biomacromolecules* **12**, 4121–4126 (2011).
32 Kawai, T., Ohtsuki, C., Kamitakahara, M., Miyazaki, T., Tanihara, M., Sakaguchi, Y. & Konagaya, S. Coating of an apatite layer on polyamide films containing sulfonic groups by a biomimetic process. *Biomaterials* **25**, 4529–4534 (2004).
33 Rhee, S.-H., Lee, J. D. & Tanaka, J. Nucleation of hydroxyapatite crystal through chemical interaction with collagen. *J. Am. Ceram. Soc.* **81**, 3029–3031 (1998).
34 Raynaud, S., Champion, E., Bernache-Assollant, D. & Thomas, P. Calcium phosphate apatite with variable Ca/P atomic ratio I. Synthesis, characterisation and thermal stability of powders. *Biomaterials* **23**, 1065–1072 (2002).
35 Isogai, A. & Kato, Y. Preparation of polyuronic acid from cellulose by TEMPO-mediated oxidation. *Cellulose* **5**, 153–164 (1998).
36 Shinoda, R., Saito, T., Okita, Y. & Isogai, A. Relationship between length and degree of polymerization of TEMPO-oxidized cellulose nanofibrils. *Biomacromolecules* **13**, 842–849 (2012).
37 Tanahashi, M. & Matsuda, T. Surface functional group dependence on apatite formation on self-assembled monolayers in a simulated body fluid. *J. Biomed. Mater. Res.* **34**, 305–315 (1997).
38 Rhee, S.-H. & Tanaka, J. Hydroxyapatite formation on cellulose cloth induced by citric acid. *J. Mater. Sci. Mater. Med.* **11**, 449–452 (2000).
39 Yokoi, T., Kawashita, M. & Ohtsuki, C. Biomimetic mineralization of calcium phosphates in polymeric hydrogels containing carboxy groups. *J. Asian Ceram. Soc.* **1**, 155–162 (2013).
40 Chi, C., Shi, Y., Zheng, H., Zhang, Y., Chen, W., Yang, W. & Tang, Y. Biomineralization process of calcium phosphate: Modulation of the poly-amino acid with different hydroxyl/carboxyl ratios. *Mater. Chem. Phys.* **115**, 808–814 (2009).
41 Zhang, R. & Ma, P. X. Biomimetic polymer/apatite composite scaffolds for mineralized tissue engineering. *Macromol. Biosci.* **4**, 100–111 (2004).
42 Takeuchi, A., Ohtsuki, C., Kamitakahara, M., Ogata, S., Miyazaki, T. & Tanihara, M. Biomimetic deposition of hydroxyapatite on a synthetic polypeptide with β sheet structure in a solution mimicking body fluid. *J. Mater. Sci. Mater. Med.* **19**, 387–393 (2008).

Supplementary Information accompanies the paper on Polymer Journal website (http://www.nature.com/pj)